General Disclaimer

One or more of the Following Statements may affect this Document

- This document has been reproduced from the best copy furnished by the organizational source. It is being released in the interest of making available as much information as possible.

- This document may contain data, which exceeds the sheet parameters. It was furnished in this condition by the organizational source and is the best copy available.

- This document may contain tone-on-tone or color graphs, charts and/or pictures, which have been reproduced in black and white.

- This document is paginated as submitted by the original source.

- Portions of this document are not fully legible due to the historical nature of some of the material. However, it is the best reproduction available from the original submission.

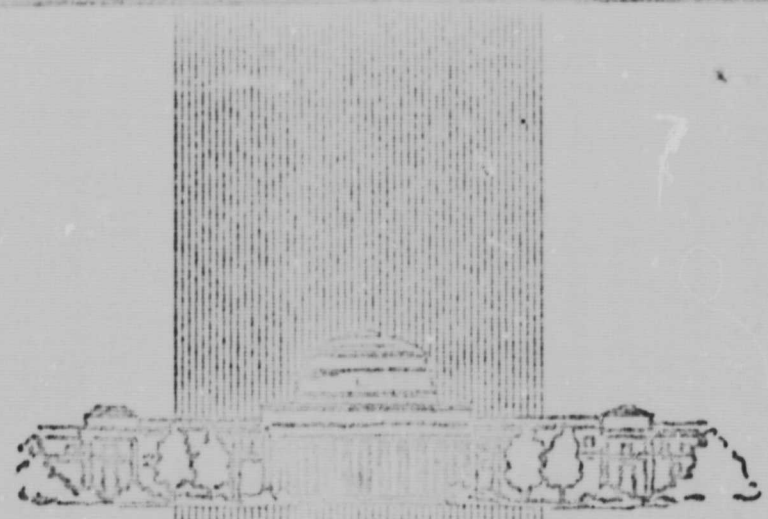

MASSACHUSETTS INSTITUTE OF TECHNOLOGY

RE-63

INVESTIGATIONS OF THE TRAPPED MAGNETIC FIELD

MEASUREMENT SYSTEMS LABORATORY

MASSACHUSETTS INSTITUTE OF TECHNOLOGY

CAMBRIDGE 39, MASSACHUSETTS

Mrs. Kenyon:

Please return this copy to me as it must be returned to Mr. H. Dolin (AERO-R)

Thanks, Lee

TABLE OF CONTENTS

ACKNOWLEDGEMENT

This report was prepared under DSR Project 71179, sponsored by the National Aeronautics and Space Administration, George C. Marshall Space Flight Center, Huntsville, Alabama through N.A.S.A. Contract NAS 8-21451.

INVESTIGATIONS OF THE TRAPPED MAGNETIC FIELD

by

Ronald R. Winters

ABSTRACT

Analytic expressions for the spatial and time behavior of trapped magnetic fields in a cylindrical conductor are found for two sets of boundary conditions. Estimates are obtained for the diffusion time in terms of the geometry of the conductor and experiments are suggested to check these estimates.

The diffusion time constant for the magnetic field trapped in a rotating aluminum disc is measured and compared with estimates obtained from solutions of Maxwell's equations. It is found that the measured diffusion times are $(2.4 \pm 0.1) \times 10^{-3}$ seconds, in fair agreement with the mathematical model. Estimates of a measure of the spatial variations in the trapped magnetic field are also obtained and compared with the physical dimensions of the apparatus.

It is shown that the temperature dependence of the diffusion time for the magnetic field trapped in a moving conductor is consistent with the temperature dependence of the conductivity of the conductor. The result is relevant to assumptions in the Babcock model of sun spots.

An experiment which studies the amplification of an azimuthal component of an initially axisymmetric magnetic field trapped in a moving conductor is described.

CHAPTER I

Calculation of the Frozen-In Magnetic Field

Introduction

Hovorka[1] has pointed out that any theory dealing with solar surface phenomena must, by nature of the physical phenomena considered, be experimentally examined in the Laboratory in a manner which isolates the various predictions and assumptions. For the past few weeks the aspect of frozen fields[2] in the Babcock theory of sunspot development has been under investigation at the M.I.T. Measurement Systems Laboratory. The experimental effort has been directed toward a fuller understanding of the diffusion of the frozen field. This report presents two calculations, based on different boundary conditions, for experimental arrangements similar to those used at the Laboratory.

Calculations

Consider the case of a conductor of conductivity σ moving through an external magnetic field restricted to some region of space V, as shown in Fig. 1-1. The conductor is a disc of diameter D and thickness b, rotating about a fixed axis through the center of the disc perpendicular to a face of the disc. We are interested in the time development of a magnetic field $\vec{B}$ which is trapped (i.e. frozen) in the disc and carried out of the region V. A coordinate system is set up as shown in Figure 1-1.

We assume that after the region of interest, A, has swept through the external field, some part $\vec{B}$ of the external field is trapped in the conductor as predicted by[2]

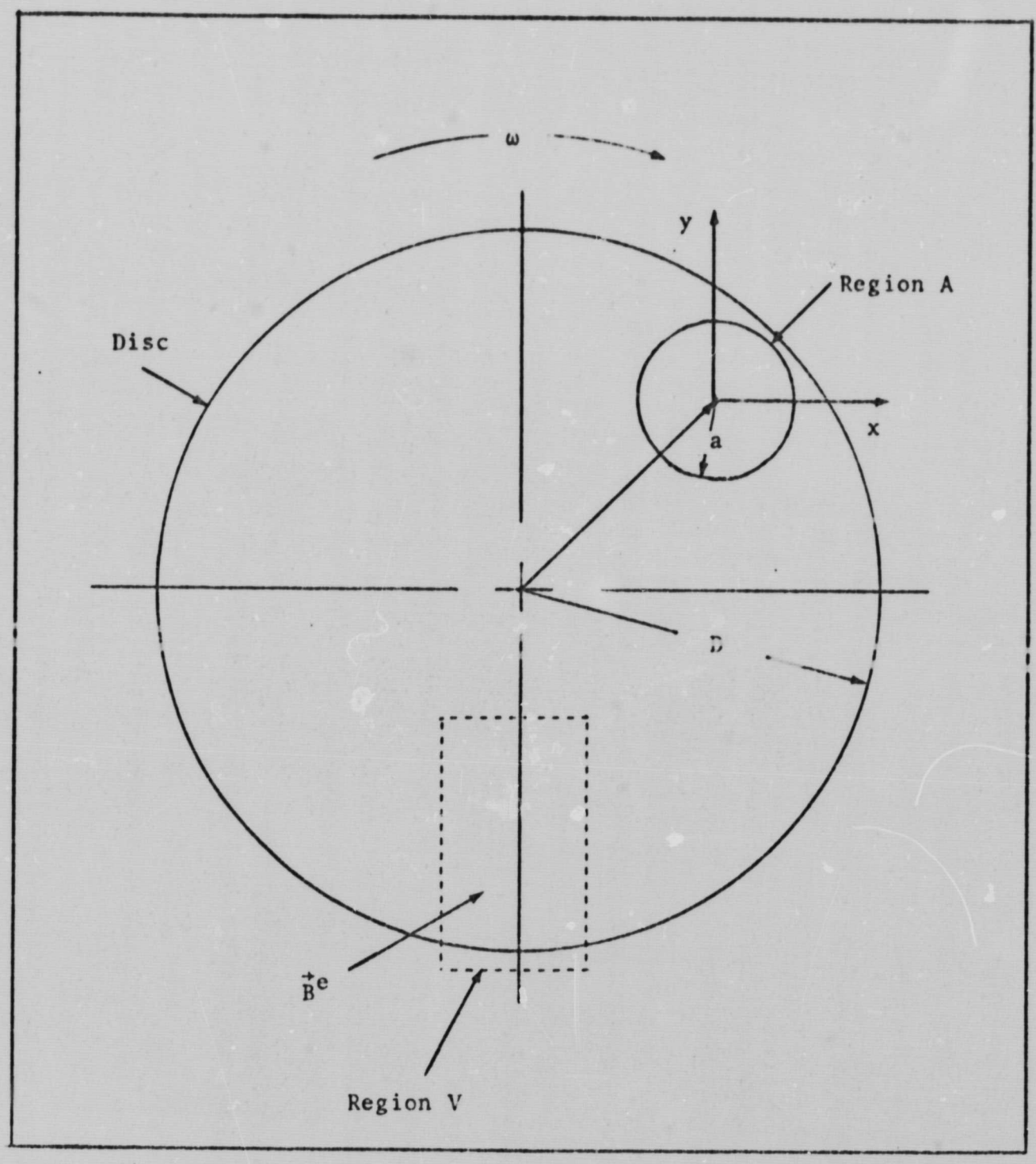

Figure 1-1
The Geometry

$$\frac{\partial \vec{B}(\vec{x},t)}{\partial t} = \vec{v} \times \vec{v} \times \vec{B}(\vec{x},t) + \frac{c^2}{4\pi\sigma} \nabla^2 \vec{B}(\vec{x},t) \qquad (1\text{-}1)$$

where $\vec{v}$ is the linear velocity of a point $\vec{x}$ on the disk. Transforming to the coordinate system (x,y,z) moving with the disk, we can write

$$\frac{\partial \vec{B}(\vec{x},t)}{\partial t} = \frac{c^2}{4\pi\sigma} \nabla^2 \vec{B}(\vec{x},t) \qquad (1\text{-}2)$$

where we assume that $v/c << 1$. Let any component of $\vec{B}$ be denoted by $\psi(\vec{x},t)$,

$$\frac{\partial \psi(\vec{x},t)}{\partial t} = \frac{c^2}{4\pi\sigma} \psi(\vec{x},t) \qquad (1\text{-}3)$$

Equation (1-3) is the diffusion equation and we shall apply standard methods in solving for $\vec{B}(\vec{x},t)$. First, the boundary conditions must be formulated.

Boundary conditions

Case I.

z: We assume the frozen-in field is constant over the width of the disk

$$\psi(r,\theta,z,t) = \psi(r,\theta,t) \qquad -b/2 \leq z \leq b/2.$$

θ: We require that ψ be a single-valued function of θ.

$$\psi(r,\theta,t) = \psi(r,\theta+m2\pi,t) \qquad m = 0,\pm1,\pm2,\ldots .$$

r: We require that $\psi(r,\theta,t)$ be finite everywhere over the region A.

Case II.

z: We require that the frozen-in field be an even function of z and reduce to zero at either edge of the disk

$$\psi(r,\theta,z) = \psi(r,\theta,-z)$$

and

$$\psi(r,\theta,\pm b/2) = 0.$$

θ: Same as Case I

r: Same as Case I.

The frozen-in field is assumed an even function of z, for simplicity. For example, a solution odd in z can be found, but this solution also vanishes at the center of the disk and its z-component would be oppositely directed on either side of z = 0. Thus the trapped field at t = 0 would be radically different from an external parent field approximately constant over the disc.

In the solution of Eq. (1-1) for the two sets of boundary conditions, it will be assumed that at t = 0 some initial spatial distribution of the trapped field exists. It is these initial conditions which must be precisely stated if anything other than general solutions are to be found. However, it will be shown that, even without precisely stating the initial conditions of the trapped field, an estimate for the diffusion time constant can be found.

Solution of Case I

We shall seek solutions of the form

$$\psi(x,t) = S(x)T(t) \qquad (1\text{-}4)$$

This substitution into Eq.(1-3) leads to

$$\frac{c^2}{4\pi\sigma}\,\frac{1}{S}\,\nabla^2 S = \frac{1}{T}\,\frac{dT(t)}{dt} \tag{1-5}$$

Setting both sides of Eq.(1-5) equal to constant $-\frac{1}{\tau}$,

$$\frac{c^2}{4\pi\sigma}\,\frac{1}{S}\,\nabla^2 S = -1/\tau \tag{1-6}$$

$$\frac{1}{T}\,\frac{dT}{dt} = -1/\tau \tag{1-7}$$

Equation (1-7) can be integrated to yield

$$T(t) \alpha e^{-t/\tau}. \tag{1-8}$$

We seek solutions to Equation (1-6) of the form

$$S(r,\theta) = R(r)\Theta(\theta) \tag{1-9}$$

which leads to (expressing ∇^2 in cylindrical coordinates)

$$\frac{r}{R}\,\frac{d}{dr}\left(r\,\frac{dR}{dr}\right) + \frac{4\pi\sigma}{c^2}\,r^2 = -\frac{1}{\Theta}\,\frac{d^2\Theta}{d\theta^2} \tag{1-10}$$

Setting each side of Eq. (1-10) equal to the constant m^2 produces two ordinary differential equations,

$$\frac{d^2\Theta}{d^2\theta} = -m^2\Theta \tag{1-11}$$

$$r\,\frac{d}{dr}\left(r\,\frac{dR}{dr}\right) + \left[\frac{4\pi\sigma}{c^2}\,r^2 - m^2\right]R = 0 \tag{1-12}$$

Equation (1-11) can be integrated to yield

$$\Theta = \Theta_0 \cos(m\theta + \delta m) \tag{1-13}$$

where m is required to be an integer by the single valuedness of $\Theta(\theta)$. Equation (1-12) is the Bessel's equation in the variable

$$\gamma r \equiv \left[\frac{4\pi\sigma}{c^2}\right]^{1/2} r$$

and, as such, has solutions (which are finite at r = 0)

$$R(r) = J_m(\gamma r) \tag{1-14}$$

The asymptotic behavior of J_m is given[3] by

$$J_m(\gamma r) \sim \sqrt{\frac{2}{\pi\gamma r}} \cos(\gamma r - 2m) \qquad \text{as } r \to \infty \tag{1-15}$$

$$J_m(\gamma r) \sim \frac{1}{2^m m} \gamma^m r^m \qquad \text{as } r \to 0 \tag{1-16}$$

Hence, the general solution to Eq. (1-3) becomes

$$\psi(x,t) = \left\{ \sum_{m=0}^{\infty} C_m J_m(r) \cos(m\theta + \delta m) \right\} e^{-t/\tau} \tag{1-17}$$

In Eq. (1-17) the set of coefficients C_m are to be determined by more nearly precise statements of the boundary conditions. It is interesting to note that the result is a superposition of spatial wave functions, all of which decay with the same time constant τ.

An estimate of τ can be arrived at as follows. We see from Eq. (1-16) that for small values of the argument of $J_m(x)$,

$$J_0 > J_1 > J_2 \text{ etc.}$$

In the Gaussian system of units the conductivity of most good conductors is $\sim 10^{-6}$ sec^{-1}; hence, the coefficient of r in the argument of the Bessel's functions has the order of magnitude, $10^{-2}/\tau^{1/2}$. If $\tau > 10^{-4}$ seconds, and if we choose $r = L$ so that the argument of Bessel's functions will satisfy $\gamma L \leq 0.5$, then we can assume that the $m = 0$ term will predominate and write

$$\frac{\psi(r=L,t)}{\psi(0,t)} \simeq \frac{J_0(\gamma L)}{J_0(0)} = J_0(\gamma L) \qquad (1\text{-}18)$$

If the ratio in the LHS is determined experimentally, then the value of the argument of $J_0(\gamma L)$ would serve as an estimate of τ in terms of L. This will be further developed below.

Case II

We return to Eq. (1-3) and seek solutions satisfying the second set of boundary conditions listed on page 6. The boundary conditions for z do not seem very meaningful physically, since clearly $\vec{B}(z=\pm b/2) \neq 0$ if the external field which induced $\vec{B}$ was non-zero at $z = \pm b/2$. However, these boundary conditions do serve to explicitly show the effects of making disk have a finite thickness b.

The separation of time and space variables result in

$$\psi(\vec{x},t) = S(\vec{x})e^{-t/\tau} \qquad \text{as before}$$

We are left with the equation

$$\nabla^2 S + \frac{4\pi\sigma}{c^2} S = 0 \qquad (1\text{-}19)$$

Using cylindrical coordinates, we have

$$\frac{1}{r}\frac{\gamma}{\gamma r}\left(r\frac{\gamma S}{\gamma r}\right) + \frac{1}{r^2}\frac{\gamma^2 S}{\gamma\theta^2} + \frac{\gamma^2 S}{z^2} + \frac{4\pi\sigma}{c^2\tau} S = 0$$

We seek a solution of the form

$$S(r,\theta,z) = R(z)\Theta(\theta)Z(z), \quad \text{and find that}$$

$$\frac{1}{r}\frac{d}{dr}\left(r\frac{dR}{dr}\right) + \frac{1}{r^2\Theta}\frac{d^2\Theta}{d^2} = -\left[\frac{1}{Z}\frac{d^2Z}{dz^2} + \gamma^2\right] \quad \text{where}$$

$$\gamma^2 = \frac{4\pi\sigma}{c^2\tau} \qquad (1\text{-}20)$$

Setting both sides of Eq. (1-20) equal to the constant λ^2 results in the two equations

$$\frac{d^2Z}{dz^2} + [\lambda^2 + \gamma^2]Z = 0 \qquad (1\text{-}21)$$

and

$$\frac{1}{rR}\frac{d}{dr}\left(r\frac{dR}{dr}\right) - \lambda^2 = -\frac{1}{r^2\Theta}\frac{d^2\Theta}{d\theta} \qquad (1\text{-}22)$$

Equation (1-21) can be integrated to yield

$$Z(z) = \cos(\lambda^2+\gamma^2)^{1/2}z \qquad (1\text{-}23)$$

Here we impose the condition that $Z(z)$ be even. Also, we have the condition that $Z(\pm b/2) = 0$, so that

$$\frac{b}{2}\left[\lambda_n^2 + \gamma^2\right]^{1/2} = (n + \tfrac{1}{2})\pi \qquad n = 0,1,2,\ldots$$

or

$$\gamma^2 + \lambda_n^2 = \frac{(2n+1)^2\pi^2}{b^2} \qquad n = 0,1,2,\ldots \qquad (1\text{-}24)$$

If Eq.(1-22) is multiplied by r^2, we have

$$\frac{r}{R}\frac{d}{dr}\left(r\frac{dR}{dr}\right) - \lambda_n r^2 = -\frac{1}{\Theta}\frac{d^2\Theta}{d\theta} \qquad (1\text{-}25)$$

Equating both sides of equation (1-25) to the constant m^2 results in the two ordinary differential equations,

$$r\frac{d}{dr}\left(r\frac{dR}{dr}\right) - (\lambda_n^2 r^2 + m^2)R = 0 \qquad (1\text{-}26)$$

and

$$\frac{d^2\Theta}{d\theta^2} + m^2\Theta = 0 \qquad (1\text{-}27)$$

Equation (1-27) can be integrated to yield

$$\Theta = \Theta_0\cos(m\theta+\delta m) \qquad (1\text{-}28)$$

where the requirement on m is a result of the single-valuedness of $\Theta(\theta)$. Equation (1-26) is known as the modified Bessel's equation, and has solutions (which are finite at $r = 0$),

$$R(r)I_m(\lambda_n r) \qquad (1\text{-}29)$$

The functions $I_m(x)$ are known as the modified Bessel functions of the first kind of order m. These functions have the asymptotic values

$$I_m(\lambda_n r) \sim \frac{1}{2^m m!} (\lambda_n r)^m \qquad r \to 0 \tag{1-30}$$

and

$$I_m(\lambda_n r) \sim [2\pi\lambda_n r]^{-1/2} e^{\lambda_n r} \qquad r \to \infty \tag{1-31}$$

Hence, the complete solution to Eq. (1-3) for these boundary conditions (Case II) can be written

$$\psi(x,t) = \left\{ \sum_{n=0}^{\infty} \sum_{m=0}^{\infty} C_{mn} I_m(\lambda_n r) \cos\left[\frac{(2n+1)^2\pi}{b} z\right] \cos(m\theta+\delta m) \right\} e^{-t/\tau} \tag{1-32}$$

where

$$\lambda_n^2 = \frac{(2n+1)^2\pi^2}{b^2} - \frac{4\pi\sigma}{c^2} .$$

The coefficient C_{mn} must be determined by more precisely stated boundary conditions.

An estimate of the diffusion time τ can be made in exactly the manner of Case I. Such an approach leads to

$$\frac{\psi(r=L,t)}{\psi(0,t)} \approx \frac{I_0(\lambda_0 L)}{I_0(0)} = J_0(z\lambda_0 L) \tag{1-33}$$

where the smallest value of λ_n, $n = 0$, is used in the argument of the modified Bessel's function. In Equation (1-33),

$$\lambda_0 = \left[\frac{\pi^2}{b^2} - \frac{4\pi\sigma}{c^2\tau}\right]^{1/2} .$$

Note that if Eq.(1-24) is evaluated for n and n+1 and the differences formed, then

$$\lambda_{n+1}^2 - \lambda_n = \frac{8(n+1)}{b^2}\pi^2 \tag{1-34}$$

Hence, for b ≈ 0.5 cm, a λ_0 is the dominant coefficient.

Comparison of the Two Results

The two solutions are:

Case I

$$\psi_1(\vec{x},t) = \left\{ \sum_{n=0}^{\infty} c_m J_m(\gamma r)\cos(m\theta+\delta m) \right\} e^{-t/\tau} \tag{1-17}$$

Case II.

$$\psi_2(\vec{x},t) = \left\{ \sum_{n=0}^{\omega} \sum_{m=0}^{\infty} c_{mn} I_m(\lambda_n r)\cos(m\theta+\delta m)\cos\left[\frac{(2n+1)\pi z}{b}\right] \right\} e^{-t/\tau} \tag{1-32}$$

Note that both types of boundary conditions lead to spatial waves characterized by Bessel's functions. This is to be expected and merely reflects the cylindrical geometry assumed at the outset. Note also that in both cases (indeed for any boundary conditions) this technique separation of variables) leads to the exponential decay of the frozen field with the decay constant independent of the spatial distribution.

In essence, Case I assumes the disk to extend infinitely far in the ± z directions. If we allow b → ∞ in Eq. (1-32), we have

$$\lim_{b\to\infty} I_m\left[\frac{(2n+1)^2\pi^2}{b^2} - \frac{4\pi\sigma}{c^2}r\right] = I_m(j\gamma r)$$

but

$$I_m(jx) = j^{-m} J_m(-x)$$

or

$$\lim_{b\to\infty} I_m(\lambda_n r) = (-j)^{-m} J_m(\gamma r)$$

so,

$$\psi_2 \to \psi_1 \text{ as expected}$$

It is unfortunate that neither result allows for an unambigous determination of τ in terms of the conductivity. (However, an estimate of τ in terms of a measure of the spatial variations of the trapped field can be found.) From page 9 above for Case I, if we let K be the value of the argument of $J_0(\gamma r)$ for which

$$R \equiv \frac{\psi_1(r=L_1 t)}{\psi_1(0,t)} \simeq J_0(\gamma L) \ ,$$

then

$$L^2 \frac{4\pi\sigma}{c^2} = K^2 \ .$$

$$\tau_{\text{Case I}} \simeq \frac{1}{K^2} \frac{4\pi\sigma L^2}{c^2} \qquad (1\text{-}35)$$

Similarly, from page 11 for Case II with the same definitions of R and k,

$$\tau_{\text{Case II}} \simeq \left[1 - \frac{L^2\pi^2}{K^2 b^2}\right]^{-1} \tau_{\text{Case I}} \ . \qquad (1\text{-}36)$$

The factor L is a length characterizing the spatial variations of the trapped field. To within the approximations leading to Equations (1-35) and (1-36) the effect of the boundary condition of finite extent in the $\pm$ z directions is to lengthen the decay time.

Experiments Suggested

The above development suggests two experiments which would be useful in understanding the nature of the diffusion of the trapped magnetic field.

1. Measurement of the diffusion time[2].

It would be interesting to compare the value predicted by Equations (1-33) and (1-34) for the diffusion times with experimental measurements of the diffusion time. In particular, Eq. (1-34) predicts a lengthening of the diffusion time when the thickness of the disc is reduced. Also these predictions,coupled with measurements of the diffusion time, would result in an estimate of that length L which characterizes the spatial variations in the trapped field.

2. Study of the behavior of the diffusion time with variations in temperature of the conductor.

In both Case I and Case II we should have, for a given geometry of the experiment, diffusion time proportional to conductivity. Hence, if the conductivity of the conductor is changed,(e.g. by varying the disc temperature), the diffusion constant should change proportionally. This prediction could be checked with apparatus existing at the Laboratory.

CHAPTER II

Diffusion Time for the Frozen-Field

Introduction

An important feature of the Babcock[4] model of solar surface phenomena is trapping (freezing-in) of magnetic fields in a conducting medium. This trapped flux, which is at first nearly dipolar and axisymmetric, is distorted by the differential rotation rate of the solar plasma, producing an azimuthal component of the magnetic field. This azimuthal component is amplified until twisting of the tubes and buoyancy-effects force loops of the flux tubes to break through the solar surface, resulting in bipolar magnetic regions. Such regions are associated with sun spot activity as well as with other surface phenomena. Babcock assumed that the magnetic field was rigidly frozen into the surrounding plasma. This requirement is too stringent. It is sufficient for Babcock's model to require that the diffusion of the trapped magnetic field be slow compared to the rate of distortion of the field by the differential rotation of the plasma. A clearer understanding of the diffusion constant in terms of the conducting medium is necessary in order to examine the structure of Babcock's model.

In the present work, an attempt is made to estimate the diffusion time constant in terms of the characteristics of the conducting medium, in this case, an aluminum disc. This estimate is then compared with measurements of the diffusion time constant for a rotating aluminum disc.

Experimental Procedure

The apparatus used in this work is that discussed by Hovorka.[2] A 15-inch-diameter aluminum disk, 1/4-inch thick, was rotated about an

axis perpendicular to the plane of the disk. A small coil (about 100 turns of fine wire) of 1-inch diameter is embedded in the disk, and is carried by the rotating disk through an external magnetic field $\vec{B}^e$. The external field, ignoring fringing effects, was directed perpendicular to the plane of the disk. The effects of the external field on the disk in the region of the coil were studied via the induced voltage at the terminals of the coil. The voltage pulse as the coil was swept through the field was recorded by a recording oscilloscope CEC model 5-124. The voltage trace was recorded on Eastman linegraph direct print paper with a record speed of 64 inches/second and a writing speed of about 8×10^4 inches/second. A typical voltage pulse is shown in Figure 2-1. Note that the voltage peak corresponding to the exit of the coil from the region of the external field has a smaller value for the magnitude of the maximum voltage than the peak corresponding to the coil's entry into the external magnetic field. Also note that the exit peak of the curve decays away much more slowly than the entry peak increases. In fact, the magnetic field in the disk is non-zero even after the coil has left the region of the external magnetic field. This is taken as evidence of the trapping of a portion of the external magnetic field. The part of the peak labeled "diffusion of trapped field", then, characterizes the freezing-in of the external magnetic field.

Treatment of the Data

The oscillograms were not directly calibrated so that techniques had to be developed to convert the raw voltage record into a useful form. Direct measurements could not be made from the oscillograms because, even with the maximum available record speed (64 inches/sec.), the voltage pulse was compressed to the order of one inch along the time axis of the record.

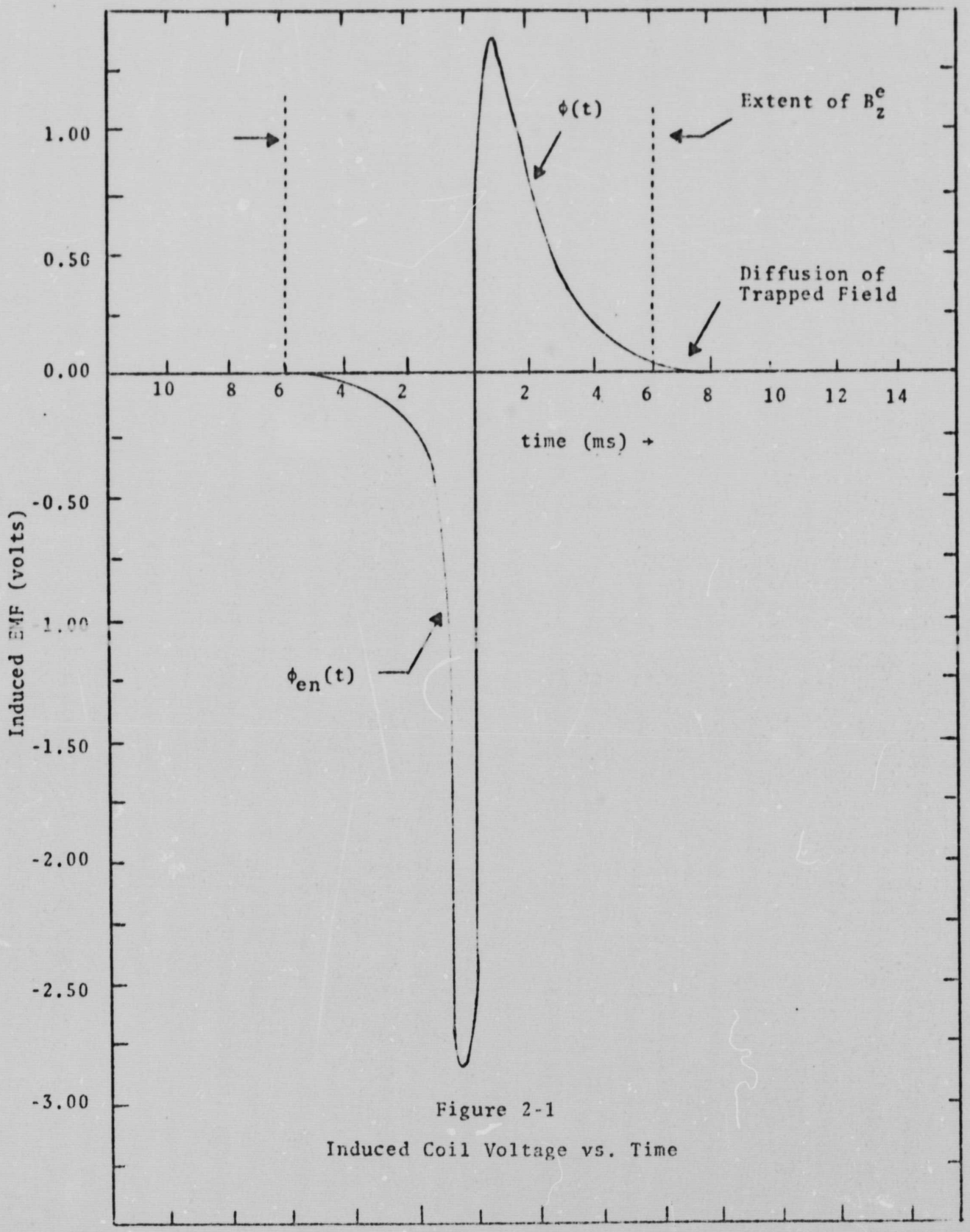

Figure 2-1

Induced Coil Voltage vs. Time

One method of treating the oscillograms is due to Hovorka[2]. This technique involved tracing over the voltage record in pencil to enhance the contrast of the trace and then projecting onto graph paper via an opaque projector. The englarged (~3x) voltage record was then traced. Unfortunately, the double-tracing procedure resulted in final voltage records which were not simply enlarged copies of the originals. In particular, the narrow voltage peaks in the entry part of the curve were difficult to trace over without some change in the apparent width of the peak. In fact, the width of the penciled curve was often about equal to the peak width in the original voltage record. However, with practice, this method was developed to a precision of about 10%.

A second method proved to be more satisfactory. In this method a photographic transparancy of the oscillogram was made using Polaroid film (type 146-I). The transparency was then projected via photographic enlarger onto graph paper. The enlarged (~2x) voltage record was then traced. This method eliminated one of the free-hand tracings, but was plagued by the lack of contrast in the oscillograms. The zero cross-over point was not visible in the transparencies. However, this point was easily located relative to the peaks in the oscillogram. Precise measurements of the relative position of the zero cross-over resulted in the location of the zero cross-over on the enlarged tracings with an expected error of less than 2%.

Geometry

The following development will employ a cylindrical coordinate system (r,θ,z) fixed in the disc with origin at the center of the detection coil. The z axis is directed perpendicular to the plane of the disc with $z = 0$ located at the half-thickness of the disk.

Theory

The time-spatial development of the magnetic field $\vec{B}(x,t)$ in a conducting medium of conductivity can be written

$$\frac{\partial \vec{B}(\vec{x},t)}{\partial t} = \vec{\nabla} \times \vec{v} \times \vec{B}(\vec{x},t) + \frac{c^2}{4\pi\sigma} \nabla^2 \vec{B}(\vec{x},t) \qquad (2\text{-}1)$$

In Eq.(2-1), $\vec{v}$ is the velocity of the conducting medium relative to some frame of reference. If the transformation to a frame of reference moving instantaneously with velocity $\vec{v}$ is made (and $v/c << 1$), then Eq. (2-1) becomes

$$\frac{\partial \vec{B}(\vec{x},t)}{\partial t} = \frac{c^2}{4\pi\sigma} \nabla^2 (\vec{B}(\vec{x},t) \qquad (2\text{-}2)$$

The solution to Eq. (2-2) is discussed in Chapter I, and only the results will be presented here. In Chapter I, it is shown that if the "frozen field" B does not vary over the thickness b of the disk, then solutions to Eq. (2-2) have the form

$$B_\alpha(r,\theta,z,t) = \left\{ \sum_{n=0}^{\infty} C_n J_n(\beta r) \cos(n\theta + \delta n) \right\} e^{-t/\tau} \qquad (2\text{-}3)$$

where

$$\alpha = (r,\theta,z) \qquad (2\text{-}4)$$

and

$$\beta^2 = \frac{4\pi\sigma}{c^2\tau} \qquad (2\text{-}4)$$

The functions $J_n(\beta r)$ are the Bessel functions of the first kind of order n. If r is limited to values such that

$$\beta r \leq 0.5 \ , \tag{2-5}$$

then the n = 0 term in Eq. (2-3) dominates the sum so that

$$B_\alpha(r,\theta,t) \approx C_0 J_0(\beta r) \cos \delta_0 e^{-t/\tau} \ . \tag{2-6}$$

We can write

$$R(K) \equiv \frac{B_\alpha(L,\theta,t)}{B_\alpha(0,\theta,t)} \approx J_0(K) \tag{2-7}$$

where

$$K^2 = \beta^2 L^2 \tag{2-8}$$

$$L \leq \frac{0.5}{\beta}$$

Thus, an estimate for the diffusion can be written

$$\tau \approx \frac{1}{K^2} \ \frac{4\pi\sigma L^2}{c^2} \tag{2-9}$$

where K^2 must satisfy Eq. (2-5) for r = L. It was shown in Reference 2 that the form of τ is not changed by imposing a z dependence on the trapped field. Hence, in any experiment for which the trapped field is approximately independent of z, we would expect Eq. (2-9) to yield a good estimate of τ. The choice of a value for the ratio R remains very much arbitrary. All that can be said at this point is that the ratio should be chosen in such a way as to measure the spatial variation of the trapped field.

The Ratio R

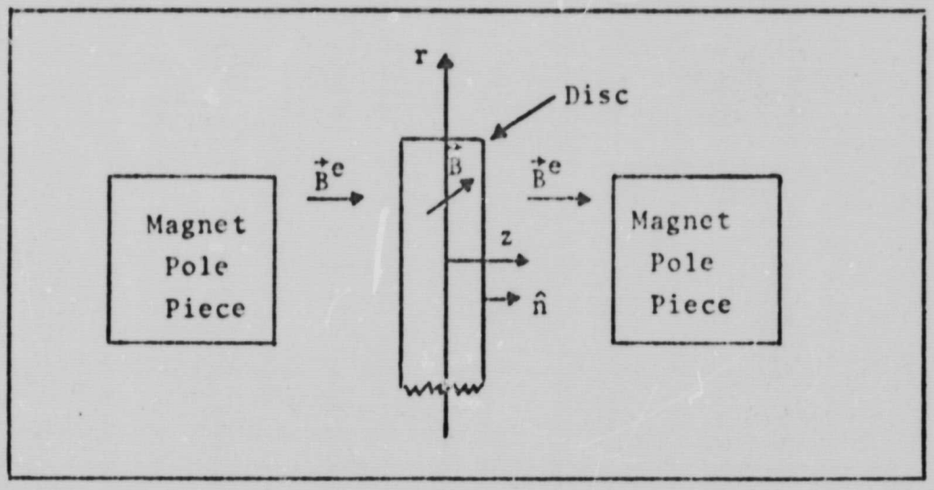

Figure 2-2

The Boundary Conditions on $\vec{B}$

Applying Gauss's theorem for the surface (See Figure 2-2) of the disc, to the equation

$$\vec{\nabla}\cdot\vec{B}(\vec{x},t) = 0$$

yields

$$[\vec{B}(r,\theta,z=\pm b/2,t) - \vec{B}^e(r,\theta,z=\pm b/2,t)]\cdot\hat{n} = 0$$

or

$$B_z(r,\theta,z=\pm b/2,t) = B_z{}^c(r,\theta,z=\pm b/2,t).$$

Thus, if the external field exhibits some spatial character over the surface of the disc, the trapped field shares that character near $z = (\pm b/2)$. For a thin disc, and an external field which is only a mild function of z over the thickness of the disc, it should be approximately true that the trapped field approximately retains the (r,θ) character of the parent external field. This assumption allows an

estimate of the ratio R to be made in terms of the external magnetic field. With this assumption Eq. (2-7) can be written

$$R(K) \equiv \frac{B_\alpha(L,\theta,z,t)}{B_\alpha(0,\theta,z,t)} \approx \frac{B_\alpha{}^e(1,\theta,z,t)}{B_\alpha{}^e(0,\theta,z,t)}$$

Thus, it is sufficient to measure the spatial variations in the external magnetic field.

The Experiment

a. Spatial Variations of the External Field.

The external field was mapped using a gaussmeter (Radio Frequency Labs model 1295) equipped with a Hall-crystal probe. The mapping was done relative to a rectangular coordinate system with origin at the center of the magnet gap. The z axis is assumed parallel to the z axis of the cylindrical coordinate system fixed in the disc (See Figure 2-3).

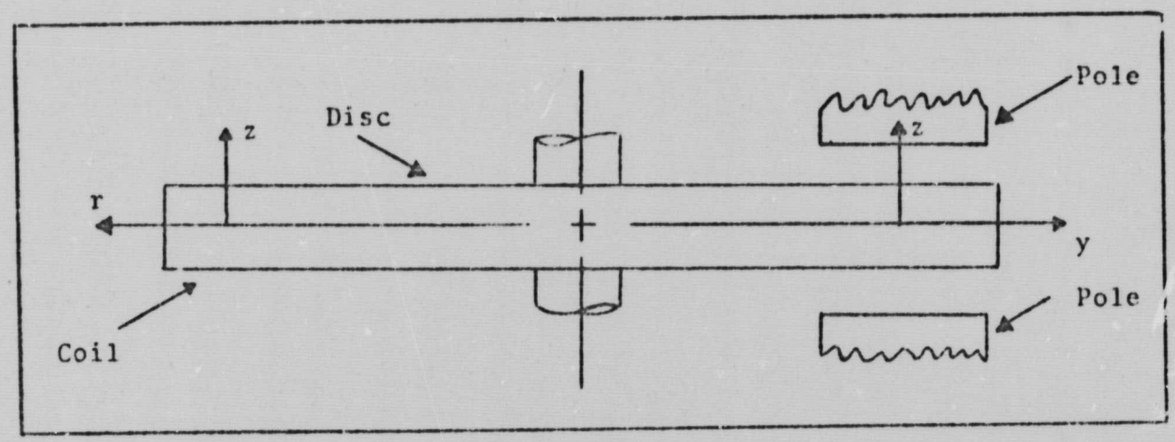

Figure 2-3

Mapping Geometry

The results of the mapping are shown in the field contours in Figures 2-4 and 2-5.

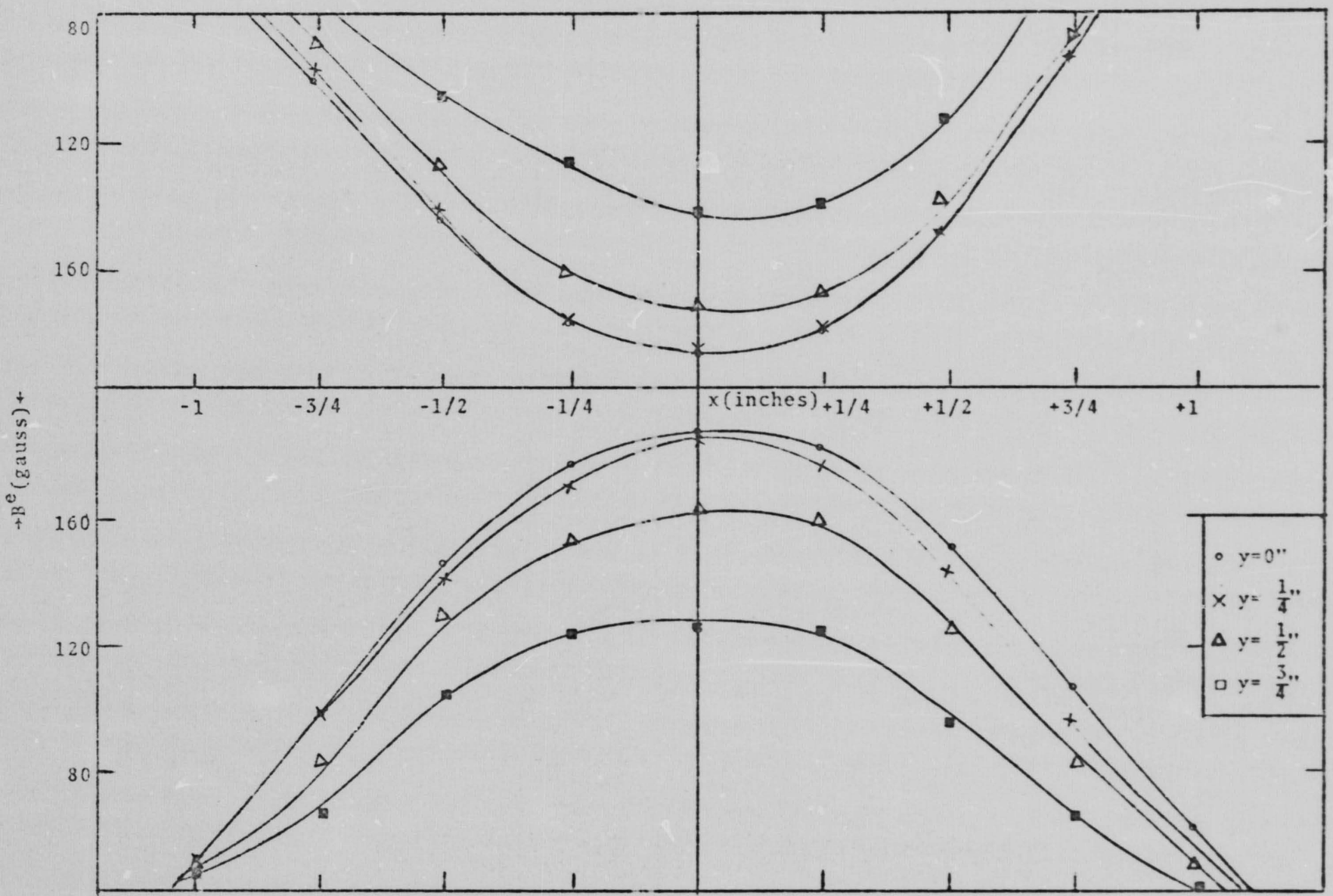

Figure 2-4

$B^e(x,y)$ vs. x

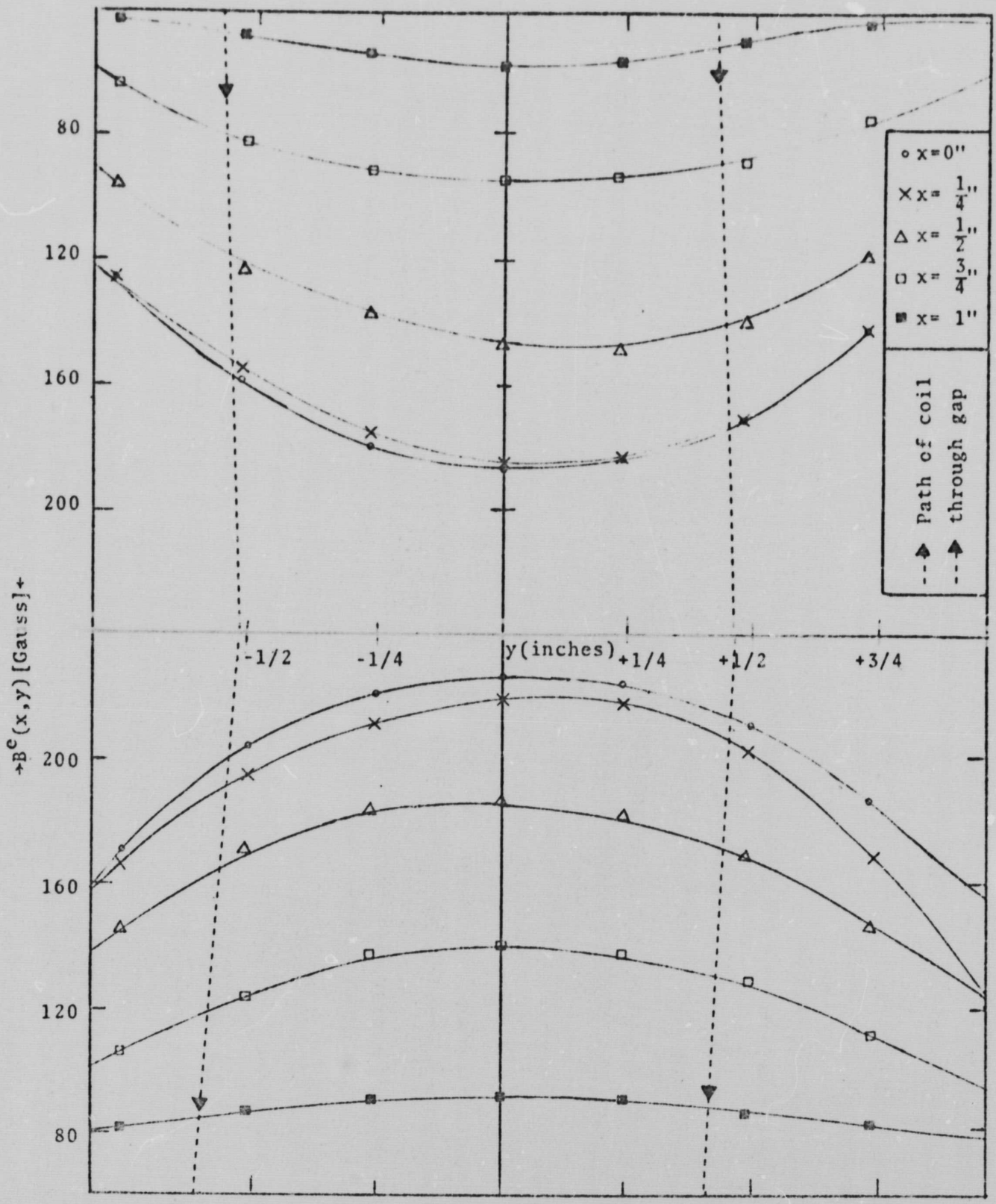

Figure 2-5.
$B^e(x,y)$ vs. y

Over the thickness of the disc, the variation in the z component of the external field was found to be less than 2%. Since this variation is within the experimental error of the measurement process, it can be assumed that the z component of the external field is constant over the thickness of the disc. Thus, if it is assumed that the spatial characteristics of the z component of the trapped field are the same as those of the external field, the solutions corresponding to Case I of Chapter I should be applicable.

It was found that the spatial behavior of the external magnetic field would be described by a form

$$B^e(x,y) = a_0 + a_1y + a_2yx + a_3y^2 + a_4x^2 + a_5y^2x + a_6yx^2 + a_7y^2x^2 + a_8x^4. \quad (2\text{-}10)$$

The coefficients in Eq. (2-10) were evaluated by forcing the function to pass through nine experimentally determined values of the external magnetic field. The values of the coefficients are given in Table 2-I.

a_0	a_1	a_2	a_3	a_4	a_5	a_6	a_7	a_8
186	11	14	-74	-191	-3	-20	55	55

Table 2-I

Values of the Coefficients in Eq. (2-10).

Table 2-II presents an estimate of the goodness of this fit by comparing experimentally determined values of the external field with those calculated from Eq. (2-10). The fit is by no means perfect, but should be good enough for the job at hand, i.e. for the estimation of R.

(x,y) Inches	$B_z^e(x,y)$ Calculated	$B_z^e(x,y)$ Experimental	Difference
(0,0)	186 gauss	186 gauss	0 gauss
(0,1/4)	174	183	9
(0,1/2)	141	143	2
(0,3/4)	96	96	0
(0,1)	50	59	9
(3/4,0)	152	142	10
(1/2,0)	174	173	1
(1/4,0)	184	180	4
(-1/4,0)	178	183	5
(-3/4,1)	58	41	17
(0,-1)	50	50	0
(-1/2,-1)	58	47	11

Table 2-II

Comparison of Fitted Function with Measured Values of External Field

b. Estimation of the Ratio R

If the initial trapped field retains the symmetry of the external field, then from Eq.(2-7) we can estimate the ratio R by

$$R \approx \frac{B_z^e(L,0,z,t)}{B_z^e(0,0,z,t)} \qquad (2\text{-}11)$$

Transforming Eq. (2-10) to cylindrical coordinates, and assuming that the maximal field is trapped as the center of the coil is coincident with the center of the gap, we can write for the value of R

$$R \approx \frac{186+11L\sin\theta+14L^2\sin\theta\cos\theta-74L^2\sin^2\theta-191L^2\cos^2\theta}{186} \qquad (2\text{-}12)$$

In Eq. (2-12) terms of the order L^3 have been neglected. Values of R for a few values of θ are given in Table 2-III.

θ	R*
0 rad.	$1.00 - 1.03L^2$
$\pi/2$	$1.00 + 0.06L - 0.40L^2$
π	$1.00 - 1.03L^2$
$3\pi/2$	$1.00 - 0.06L - Q.40L^2$

Table 2-III

The Ratio R

*Note: L must be expressed in inches in this case.

c. A Value for L

We require that L be a measure over which the spatial variation in the external field is R. If we arbitrarily set R = 0.95 and 0.90, the following values for L are found.

R \ L	θ=0 rad,	$\theta=\pi/2$	$\theta=\pi$	$\theta=3\pi/2$
0.95	0.6cm	1.1cm	0.6cm	0.7cm
0.90	0.8cm	1.4cm	0.8cm	1.1cm

Table 2-IV

L Values

R	L
0.95	0.7cm
0.90	1.0cm

Table 2-V

L Values

As expected from the approximate azimuthal symmetry of B_z^c, the value of L is not strongly dependent on θ. Hence, Table 2-V gives the value of L averaged over θ for each value of R.

d. Calculation of Estimate of τ.

From Eq. (2-9), we can estimate τ by

$$\tau \approx \frac{1}{K^2} \frac{4\pi\sigma L^2}{c^2}$$

where K satisfies Eq. (2-5) and

$$R(K) \approx J_0(K) .$$

The data given in Table 2-VI are taken from the Handbook of Tables for Mathematics.

$R \approx J_0(K)$	K	L	$J_1(K)$
0.95	0.40	0.7cm	0.20
0.90	0.60	1.0cm	0.29

Table 2-VI

Parameters for Calculation of τ

Note that K just satisfies Eq. (2-5) for R = 0.95 and just exceeds the bound established by Eq. (2-5) for R = 0.95. (Compare J_0 with J_1 in Table 2-VI). Using $\sigma = 2.7 \times 10^{-7}$ sec^{-1} for commercial aluminum, the following estimates were calculated for the diffusion constant.

R	K	L(cm)	τ(ms)
0.95	0.40	0.7cm	1.2ms
0.90	0.60	1.0cm	1.0ms

Table 2-VII

Calculated Diffusion Constant

Hence, the mathematical model predicts a diffusion time constant of the order of 10^{-3} seconds.

e. Experimental Determination of τ.

As has already been pointed out, Figure 2-1 shows that the voltage pulse does not go to zero as the coil leaves the region of non-zero external field. The resultant voltage curve (labeled $\phi(t)$ in Figure 2-1) as the coil leaves the region V is a result of two effects; one, the rate of change of the external field and, two, the rate of change of the trapped flux. We can write

$$\phi(t) = \phi_e(t) + \phi_f(t)$$

where

$\phi_e(t) \equiv$ voltage due to changes in external field as the coil exits from V.

$\phi_f(t) \equiv$ voltage due to changes in the trapped flux in the region A.

The external magnetic field has been shown[2] to be nearly symmetric with respect to the coil's entry into and exit from the region V. Hence, it should be approximately true that in the absence of trapping of the field,

$$\phi_{en}(t) = -\phi_e(-t)$$

where $\phi_{en}(t) \equiv$ induced voltage as coil enters V. Thus, we can write

$$\phi_f(t) = \phi(t) + \phi_{en}(t) \tag{2-13}$$

Now, Faraday's law implies

$$\phi_f(t) = -\frac{1}{c}\int_A \frac{\partial \vec{B}}{\partial t}\cdot\hat{n}\, da \tag{2-14}$$

$$\phi_f(t) = \frac{1}{c\tau}\left\{\int_A S_z(r,e,z)da\right\}e^{-t/\tau} \tag{2-15}$$

where S_z is the z component of the trapped field (Eq. (2-3)). Thus, we can write

$$\ln\phi_f(t) = -\frac{t}{\tau} + \text{constant} \tag{2-16}$$

Figure 2-6 presents a typical plot of $\phi(t)$ for data taken with the disk rotating at 1700 rpm. The slope of the fitted straight line, results in the measured value for τ.

$$\tau = (2.4 \pm 0.1) \times 10^{-3} \text{ seconds.}$$

Conclusions

The measured decay constant is about twice the estimated value. This would imply that the length L has been underestimated by Eq. (2-11). However, the approximate agreement indicates that the trapped field

does approximately retain the spatial characteristics of the parent external field. Also, it is clear thet the parameter L (for this experiment) is of the order of one half the radius of the detection coil.

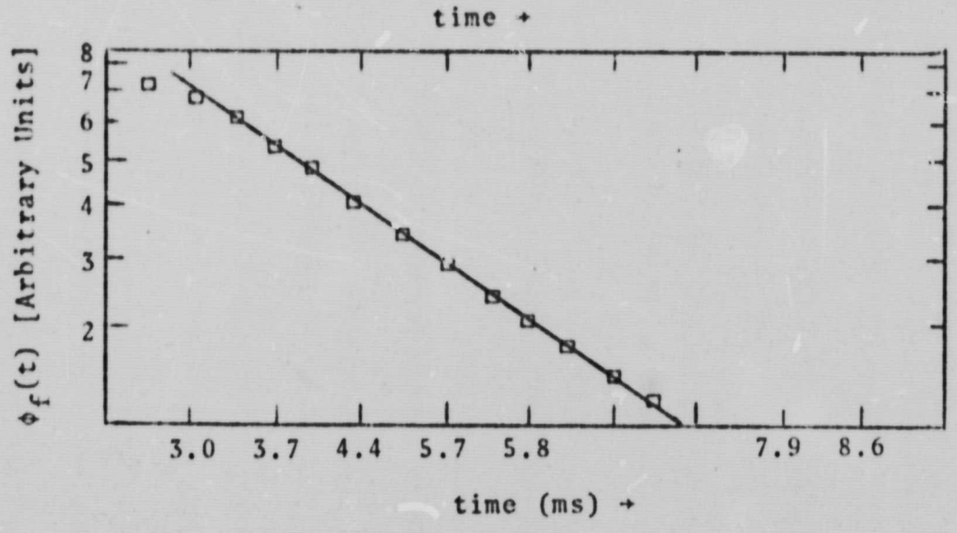

Figure 2-6

Decay of the Trapped Flux

CHAPTER III

Temperature Dependence of the Trapped Flux Diffusion Time

Introduction

This chapter continues the discussion of the nature of the diffusion of a magnetic field trapped in a rotating aluminum disc. The impetus for the study is a paper by Babcock[4] in which a model for solar surface bipolar magnetic regions is presented. One of the essential features of this model is the assumption that the solar plasma (to the depth of 0.1 R_θ) has great enough conductivity to trap (freeze-in)[5] the magnetic field. It has been shown[5] that the diffusion time of the trapped field should be proportional to the conductivity. The present work was undertaken to test this prediction and the assumptions leading to it.

Experimental Procedures

The conducting medium for this and other work was a 15 inch diameter aluminum disc which rotated about an axis perpendicular to the plane of the disc. A one inch diameter coil of 100 turns of fine wire was embedded in the disc. The center of the coil was located at the half-thickness about 6 1/2 inches from the center of the disc. The coil was carried by the rotation of the disc through a magnetic field of about 150 gauss. Chapter 2 discussed the geometry of the field. The conductivity of the disc was varied by varying the disc temperature. The temperature was monitored by a thermocouple clamped tightly to the disc in the vicinity of the coil. The disc temperature was varied about room temperature by two methods. First, the disc was cooled to about 10°C and then, while approaching thermal equilibrium with the room, measurements of the diffusion time were made. For temperatures above ambient temperature, the disc was heated to about 120°C and measurements

of the diffusion times were made as the disc cooled to room temperature. Diffusion times were measured over a temperature span of about 33°C. The diffusion of the magnetic field was detected by the voltage induced at the terminals of the coil. A typical voltage pulse is shown in Figure 2-1.

The voltage records were recorded by a recording oscilloscope with a record speed of 64 inches/second and a writing speed (with Kodak Direct Print Paper) of about 8×10^5 inches/second. As shown by Figure 2-1, the voltage pulse is asymmetrical about the zero cross-over (defined to occur at time $t = 0$). The quantities appearing in Figure 2-1 are defined by:

$\phi(t) \equiv$ induced voltage as the coil recedes from the external magnetic field.

$\phi_{en}(t) \equiv$ induced voltage as the coil enters the external magnetic field.

$\phi_e(t) \equiv$ induced voltage expected if there were no magnetic flux trapped as the disc moves out of the external field.

If, as in the present work, the geometry of the coil's encounter with the external magnetic field is symmetric with the coils exit from the field[2], then one would expect that, in the absence of trapping of the external field,

$$\phi(t) = - \phi_{en}(-t)$$

Clearly this is not the case. The diffusion time of the trapped field is long enough so that an appreciable voltage is induced for about a millisecond after the coil leaves the external field. The induced voltage $\phi(t)$ is due to two effects, one the rate of change of the external

field and, two, the rate of change of the trapped flux. We can express this as

$$\phi(t) = \phi_e(t) + \phi_f(t) \tag{3-1}$$

where

$\phi_f(t)$ = the voltage induced by the decay of the trapped field.

Since, in the absence of trapping, we expect symmetry in the induced voltage with respect to entry into and exit from the external field, we require

$$\phi_e(t) = - \phi_{en}(-t) \tag{3-2}$$

Thus, the induced voltage due only to the diffusion of the trapped flux can be written

$$\phi_f(t) = \phi(t) + \phi_{en}(t) \tag{3-3}$$

Equation (3-3) allows the effects of diffusion to be calculated from the voltage record (Figure 2-1).

Since the diffusion is assumed[2] to be exponential with diffusion constant τ, we can write for the z component of the trapped magnetic field

$$B_z(r,\theta,t) = S_z(r,\theta)e^{-t/\tau} \tag{3-4}$$

where S_z is the spatial functional dependence of the z component of the trapped field in the region of the coil. Now, the induced voltage can be expressed

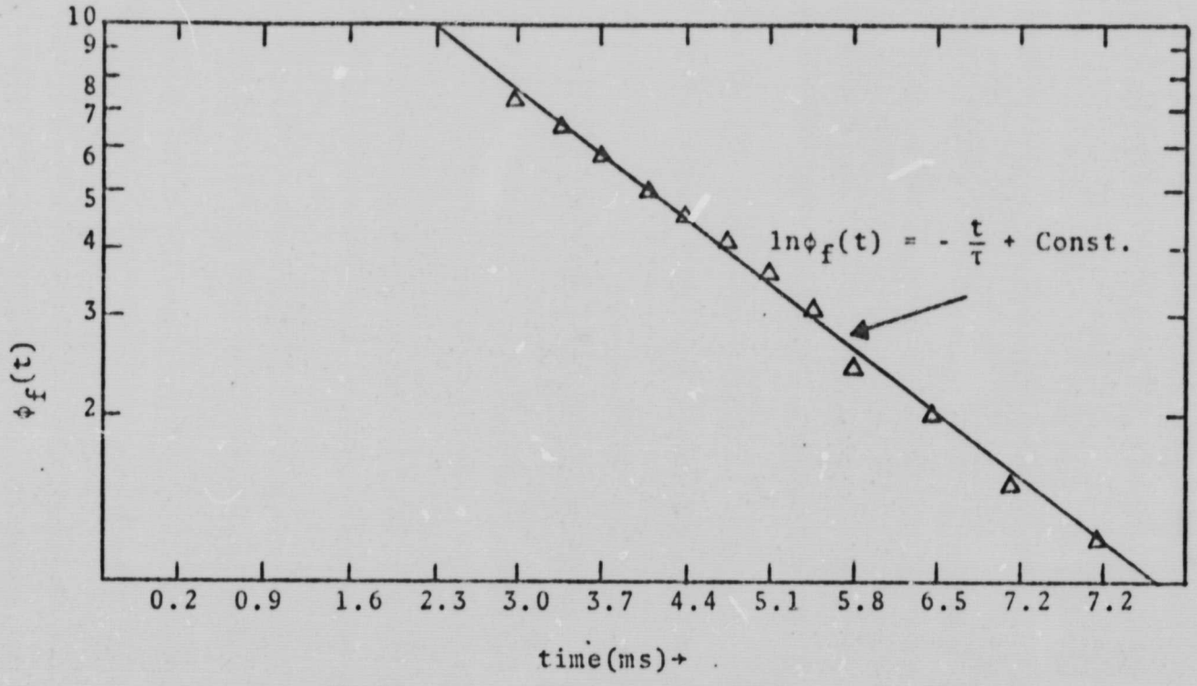

Figure 3-1. Semilog Plot of ϕ_f vs. Time

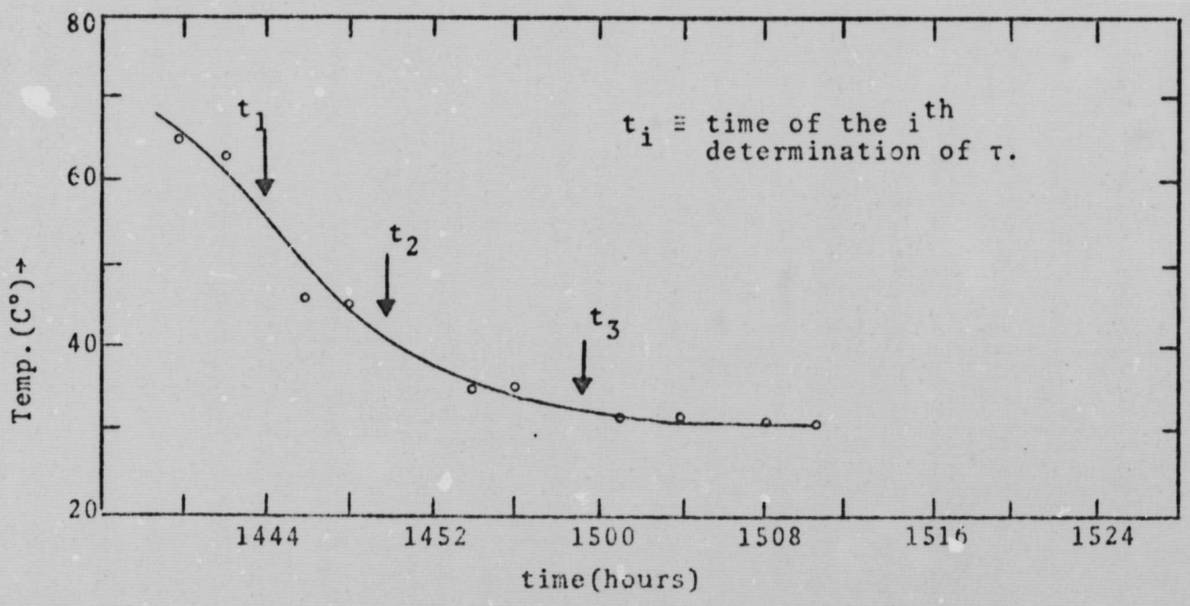

Figure 3-2. Temperature of Disc vs. Time

$$\phi_f(t) = -\frac{1}{c}\int_A \frac{\partial \vec{B}}{\partial t}\cdot\hat{n}\, da$$

where $\vec{B}$ ≡ trapped magnetic field

A ≡ area of the coil

n ≡ unit vector perpendicular to plane of disc and coil.

$$\phi_f(t) = \frac{1}{c\tau}\left\{\int_A S_z\, da\right\} e^{-t/\tau} \qquad (3\text{-}5)$$

or

$$\ln \phi_f(t) = -t/\tau + \text{constant} \qquad (3\text{-}6)$$

Figure 3-1 presents a typical semilog plot of $\phi_f(t)$ versus t. The fact that most of the data lie nearly on a straight line supports the assumptions leading to Eq. (3-6). The slope of the line drawn through the data provides the measured value of τ.

As stated earlier, the diffusion times were measured at various times, and therefore different temperatures, as the disc approached thermal equilibrium with the room. The temperature of the disc could be monitored only when it was not rotating. Thus, the disc temperature for each determination of τ was estimated by interpolation of temperature data obtained before and after each measurement of τ. Figure 3-2 presents the temperature data for a typical series of diffusion time determinations. The curve drawn through the data in Figure 3-2 was used for estimating the temperature at the various times t_i.

Table 3-I presents the measured values of the diffusion time for various temperatures.

τ(ms)	Temp° C
2.19 ± 0.13	56°C
2.24 ± 0.09	41
2.46 ± 0.18	33
2.43 ± 0.07	28
2.50 ± 0.09	23

Note: the errors quoted are in Table I and represent the probable errors of the measurements.

Table 3-I

Diffusion Times for Various Temperatures

The resistivity of commercial aluminum can be represented[6] by

$$\zeta(T) = 1 + \alpha_0 T \times 10^{-3} \qquad (3\text{-}7)$$

where $\alpha_0 = 4.0$. As stated earlier the diffusion time should be proportional to the conductivity or inversely proportional to the resistivity.

$$\tau(T) \propto \frac{1}{\zeta(T)}$$

If we let T_1 be some temperature such that $T < T_1 < 0$, then

$$\frac{\tau(T)}{\tau(T_1)} = 1 - \alpha_0[T-T_1] \times 10^{-3} \qquad (3\text{-}8)$$

Figure 3-3 presents a plot of the measured diffusion times (Table 3-I) versus temperature. Equation (3-8) was forced to pass through the data at $T_1 = 23°C$ and is shown as the line drawn through the data in Figure 3-3.

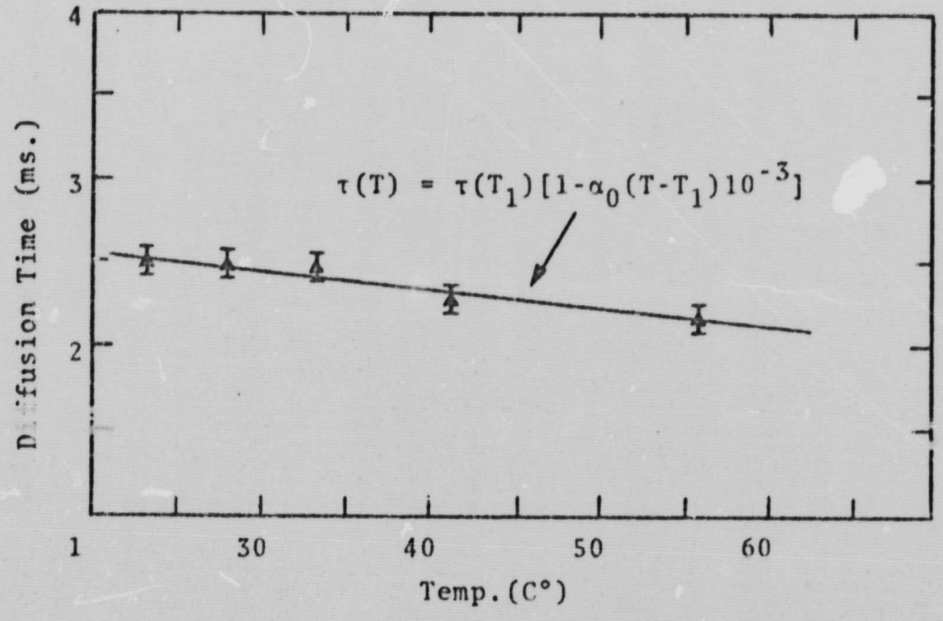

Figure 3-3. Diffusion Time vs. Temperature

Conclusions

The diffusion time of the trapped field displays a temperature dependence which is consistent with that expected of the conductivity. This result is consistent with the assumption that the diffusion time of the trapped field is proportional to the conductivity of the medium.

CHAPTER IV

Amplification of the Frozen-In Magnetic Field

Introduction

In Babcock's[4] model of the sun's magnetic field, the developement of a toroidal field from the initial dipolar field results in the production of the bipolar magnetic regions (BMR) associated with sunspot activity. The model pictures the toroidal field as being produced by distortion of the dipolar field at depths of about 0.1R by the differential rotation of the solar plasma. The dipolar field is imagined trapped in (frozen into) the plasma and carried with it. The toroidal field is produced and amplified as the trapped field is wrapped around the rotation axis of the sun. Ultimately, as a consequence of twisting, loops are formed in the toroidal field. When these loops become buoyant enough, they break through the solar surface resulting in the BMR's associated with sunspot activity. Babcock's model rests heavily on the supposition that if initially an axisymmetric magnetic field is trapped in a differentially rotating conducting medium, the trapped field will be distorted and the distortions amplified.

A great deal of work[7,8,9,10,11] has been undertaken to study the effects of an external field on a rotating conducting medium. Surprisingly, no reference can be found of work done to detect the inverse effect, that is, to detect the distortions of the magnetic field by the rotation of the conducting medium. It is this latter effect that is vital to Babcock's model and which Hoyorka and the author propose to study in laboratory experiments.

The Experiment

It is proposed to study the distortion of an initially axisymmetric

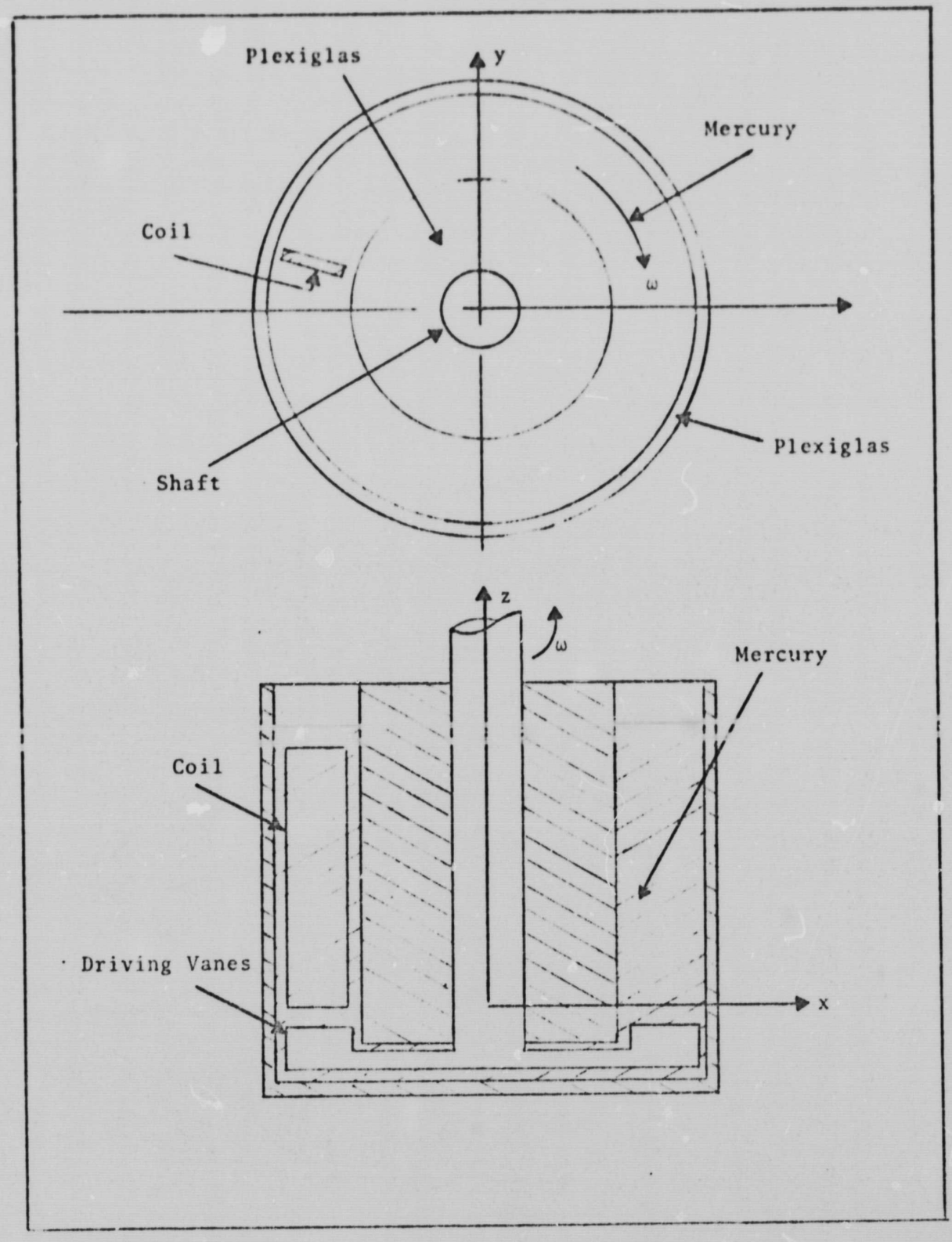

Figure 4-1

Top and Section View
of Rotating Mercury Annulus

magnetic field by the differential rotation of an annulus of mercury.

As shown in Figure 4-1, an annulus of mercury will be given a rotational velocity $\vec{\omega}(z)$; the z-dependence of the velocity will be such that a velocity gradient in the mercury will be set up along the axis of rotation z. The rotational velocity of the driving rotor (Fig. 4-1) will be slowly increased and the presence of an increase in an azimuthal component of the trapped field will be detected by a coil oriented as shown in Figure 4-1. Thus, any distortion of the initial axisymmetric field producing a field component perpendicular to the plane of the coil, will result in an induced voltage at the terminals of the coil.

Conditions Required

If the differential rotation of the mercury produces a "twist" in the frozen-in field of an amount $\Delta\phi$, this twist will be transported in the z direction at the magnetohydrodynamic speed[8]

$$V = \frac{\beta}{(4\pi\rho\mu)^{1/2}}$$

where

β: the magnetic field strength

ρ: density of mercury

μ: magnetic permability of mercury

The differential rotational speed $\Delta\omega = \omega(z = 0) - \omega(z > 0)$ must be about equal to the speed of twist-transport V is an amplification of the azimuthal component is to take place, thus,

$$\Delta\dot{\omega} \simeq \frac{\beta}{(4\pi\rho\mu)^{1/2}} \simeq \frac{1}{2} \text{ cycle/second}$$

for the physical parameter pertinent to the present experiment. Such a rotation rate is easily attained and, in fact, studies[9] of the effects of the magnetic field on the rotation of mercury at about these rotational speeds have been reported.

Status of the Experiment

Preparations for the proposed experiment have been completed. Drawings for the apparatus have been submitted and the machine shop work started. A system to vary the speed of the driving rotor synchronously with the recording of the coil voltage is yet to be designed and built.

BIBLIOGRAPHY

1. Hovorka, J., "Planet-Sun Position Correlation with Solar Activity", RN-51, Monthly Report for Nov. 1968.

2. Hovorka, J., "Experimental Demonstration of Flux-Trapping in a Moving Conductor", RN-56, July, 1969.

3. Hildebrand, F., Advanced Calculus for Applications, p. 151.

4. Babcock, H.W., "The Topology of the Sun's Magnetic Field and the 22-Year Cycle", Astrophysical Journal (133) 1961.

5. Alfven and Fathamman, Cosmical Electrodynamics, pp. 80-81, Oxford at the Clarendon Press, 1963.

6. International Critical Tables on Numerical Data, Physics, Chemistry, and Technology, Vol. VI, p. 102, McGraw Hill Book Company.

7. Lehnert, B., "On the Behavior of an Electrically Conductive Liquid in a Magnetic Field", Ark. F. Fys. (5) p. 69, 1951.

8. Falthammar, Carl-Gunne, "Experiments on Magnetohydrodynamic Co-rotation in Mercury", Ark. F. Fys. (19) p. 109, 1960.

9. Lehnert, B., "An Instability of Laminar Flow of Mercury Caused by an External Magnetic Field", Proc. Roy. Soc. A, (233), p. 299, 1955.

10. Lundquist, S., "Experimental Investigations of Magnetohydrodynamic Waves", Phys. Rev. (76) p. 1805, 1949.

11. Lehnert, B., "Experiments on Non-Laminar Flow of Mercury in Presence of a Magnetic Field", Tellus (4) p. 647, 1952.